

CRACK FORMATION UNDER HYGRAL OR THERMAL GRADIENTS

A.M. Alvaredo,
Laboratory for Building Materials,
Swiss Federal Institute of Technology Zurich

Abstract

An approach towards the consideration of stresses induced by temperature or moisture distributions including diffusion analysis and cracking is succinctly described. The material properties required for the numerical analysis, which can be either determined experimentally in a direct way or obtained by means of inverse analysis, are also dealt with. Some applications of the developed model to the time-dependent behaviour of drying concrete members are presented. It is shown that the length change of concrete specimens observed during shrinkage tests cannot be considered as a material property. Rather, it must be understood as the complex response of the specimen to a time-dependent, highly non-linear state of eigen-stresses. The effect of the slab depth on the warping of members exposed to drying at their top surface as well as of the concrete quality on the restraint reaction in dowelled slabs is also outlined. The main conclusion is that practical cases with requirements for high performance and the optimization of design or technological measures can only be treated efficiently by means of a rational approach as the one presented in this work.

1 Introduction

In 1951, while monitoring the daily and seasonal variations in the warping of concrete pavements in California, Hveem (1951) reported on a particularly interesting profile: the one corresponding to a roadway lined with a grove of eucalyptus. The general lack of flatness recorded during the measurements was in this case much less pronounced than for the rest of the pavements. It was apparent for him that the moisture drawn by the roots of the trees was the cause of this improved performance.

Many publications documenting today's state-of-the art in the design, evaluation and rehabilitation of concrete pavements emphasize the need for taking the stresses induced by temperature or moisture changes into consideration. Saxena and Dounias (1986) and Mirambell (1990) found that thermal loads in such structural elements are at least of the same order of magnitude as traffic loads. Poblete et al. (1990) conducted systematic measurements in the Chilean in-service network of undowelled plain concrete pavements during three years; the upward warping of the slabs became evident from the changes in slab deflection and in transverse joint openings. Their results showed that the deformations induced by moisture variations are as important as those due to temperature changes and that the moisture distribution throughout the depth of the slabs remained highly non-linear during the whole period under investigation.

A study of the widely used design manuals carried out by Saxena and Dounias (1986) indicates that the only stress incorporated in the pavement design is that due to wheel loads. Environmental loads are considered only indirectly by reducing the strength of the supporting subbase-subgrade system. The same holds true for the design of concrete industrial ground floors (Concrete Society, 1988). The design philosophy regarding the consideration of warping stresses is to create joints in the slab to compensate for such stresses and to base the design stress upon load alone. As pointed out by Zollinger and Barenberg (1989), this design philosophy involves a severe drawback: since warping stresses are in turn a function of the joint spacing, the optimum joint spacing cannot be rationally selected unless warping stresses are included in the total stress calculation.

The neglect of the state of stress induced by non-uniform temperature or moisture distributions in the standards and codes of practice has led practitioners to resort to merely empirical approaches. These solutions can be expected to be successful only in cases not too different from those for which experience was gained or when comparable time intervals are considered. Empirical solutions fail, however, when it is necessary to meet requirements for high performance, e.g. ensure "super-flatness" of an industrial ground floor (Holland, 1995), or to weigh the effect of one design variable or technological measure against the effect of others in a rational manner. For instance: is it justified to assume, as stated by Eisenmann and Leykauf (1990) and in the state-of-the-art report of the British Concrete Society (Concrete Society, 1988), that warping induced by environmental loads can be reduced by increasing the slab depth or, as stated by Silfverbrand (1990), by increasing the curing period? Rollings' (1989) statement that the source of the increased warping exhibited by slabs of fibre reinforced concrete is open to debate, is it still valid today?

A pioneering attempt at a rational analysis of shrinkage stresses in concrete was made by Pickett (1946). More recently, Gustafsson and Hillerborg (1984) tried to assess the influence of shrinkage-induced eigenstresses on the flexural strength of concrete beams by means of fracture mechanics considerations. Wittmann and Roelfstra (1980), Acker et al. (1990) and Acker and Eymard (1992), among other authors, proposed to analyse the volume changes experienced by concrete subjected to moisture variations by first calculating the time-dependent moisture distribution. This is the approach followed in the sequel.

Based on the work carried out by Pihlajavaara (1965) and Bažant and Najjar (1971), the theory of non-linear diffusion with a concentration dependent diffusion coefficient has been adopted for the prediction of the moisture distributions in drying concrete members. Under the assumption that coupling between water transport and the state of stresses can be neglected (see, for example, Wittmann, 1995), a stress analysis including crack formation is subsequently carried out. The numerical model will be briefly described in Section 2. The required material parameters will be outlined in Section 3. Further details of the implemented solution as well as of the experimental validation of the model by means of shrinkage tests

can be found in Alvaredo (1994). The application of the developed model to the prediction of the warping of concrete ground floors as influenced by several design variables and technological measures is dealt with in Alvaredo and Wittmann (1995a, 1995b). Some typical results will be shown in Section 4. In another contribution to this volume (Alvaredo et al., 1995), numerical results of shrinkage-induced warping are compared with experimental observations.

Although this work is concerned with concrete members under moisture gradients only, the same methodology can be applied to the analysis of stresses induced by temperature changes. Heat transport differs from moisture transport, however, in several aspects. One of them is that, as has been already recognized many years ago (Pihlajavaara, 1965), the hygral diffusion coefficient depends on moisture content in a strongly nonlinear way. Further, as will be shown in Section 3.2, infinitesimal shrinkage is also a function of relative humidity. In addition, the time scale of both processes differs in several orders of magnitude. Five distributions of relative humidity and temperature are shown in Figs. 1a and 1b, respectively. For the hygral analysis, it was assumed that the initially saturated, 25 cm thick, concrete member was exposed to an environment at 50% relative humidity at one of its surfaces. For the thermal analysis, the initial temperature was set to 40 C while the convective boundary conditions were defined by an environmental temperature equal to 0 C and a film coefficient of 0.5 m/h. The chosen hygral and thermal diffusion properties characterize the behaviour of normal concrete. As can be seen in Figs. 1a and 1b, the distribution of relative humidity after 5 years of drying is comparable to the thermal distribution after 6 hours of cooling.

2 The numerical model

Firstly, the time-dependent distribution of relative humidity in concrete members is calculated by means of the theory of diffusion. The relative humidity gradient, grad h , in the porous system is considered to be the driving force. Under isothermal humidity flux and assuming that neither sinks nor sources are present in the body (i.e. for mature and non-carbonating concrete), the governing equation reads:

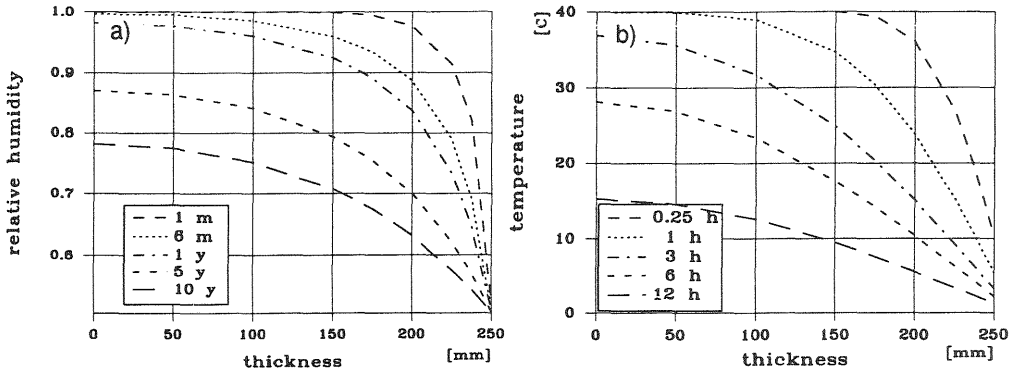


Figure 1: a) distribution of relative humidity at different durations of drying;
b) distribution of temperature at different durations of cooling

$$\frac{\partial h}{\partial t} = \operatorname{div} [D(h) \operatorname{grad} h] \quad (1)$$

where $D(h)$ represents the dependence of the diffusion coefficient on the relative humidity h , a highly non-linear relationship originated by the action of moisture transport mechanisms of different efficiency.

Convective boundary conditions are imposed at the surface s in contact with air at relative humidity h_a :

$$q_s = H_F (h_s - h_a) \quad (2)$$

where q_s is the moisture flux normal to the exposed surface, H_F is the coefficient of surface hygral transfer, or film coefficient, and h_s is the relative humidity at the surface.

In order to complete the formulation of the diffusion problem, initial conditions have to be added to the differential equation and boundary conditions. Because Eq. (1) is a differential equation of first order in time, only one initial condition is required. Saturation was assumed:

$$h(x, 0) = h_0 = 1 \quad (3)$$

The dependence of the diffusion coefficient D on h makes the diffusion problem non-linear. The finite element method was used for its solution.

The shrinkage strain increment $\Delta\epsilon_s$ of an infinitesimal volume element is considered to be proportional to the locally attained change in relative humidity Δh :

$$\Delta\epsilon_s = \alpha_{sh}(h) \cdot \Delta h \quad (4)$$

in which, usually, the initial strain-free state corresponds to saturation ($h = 1$). The coefficient of shrinkage, $\alpha_{sh}(h)$, defines the amount of shrinkage strain per unit change in relative humidity Δh which a drying infinitesimal material element undergoes if it is not constrained in its movement by adjacent elements. According to the available experimental data and to the degree of accuracy desired for the numerical analysis, the coefficient of shrinkage can be assumed as a constant or as a function of the relative humidity h .

It might be speculated that the presence of cracks serving as conduits for water vapour may enhance water diffusion. If the moisture diffusion coefficient were considered to be affected by cracking, a coupled water transport-mechanical analysis should be carried out. Because of the lack of experimental evidence showing a significant influence of cracking on the rate of moisture diffusion (e.g. Wittmann, 1995), especially for the dense system of fine cracks anticipated to appear in the drying concrete members dealt with in Section 4, no coupling between moisture transport and stresses was considered in the analysis.

A smeared formulation (Bažant and Oh, 1983) of the “fictitious crack model” (Petersson, 1981) was used to describe cracking. The following properties are required to define the mechanical behaviour of the material: modulus of elasticity, E , Poisson’s ratio, ν (a typical value, $\nu = 0.2$, was used for all calculations), tensile strength, f_t , fracture energy, G_F , and the shape of the strain softening diagram.

Concrete members subjected to uni-dimensional drying are characterized by a state of constant deformation at fibres equidistant from the exposed surface, which would induce a state of constant stress in a perfectly homogeneous continuum. As soon as the tensile strength were reached, for instance, at the first row of integration points, fracture process zones would start developing simultaneously at each of them and, as a consequence, a pattern of cracks with spacing equal to the size of the finite elements would be the numerical result, irrespective of the chosen size of the finite element mesh. Except for the effect of round-off errors, this crack pattern would remain constant during the whole drying process. From the physical point of view, this is known to be completely unrealistic. From the numerical point of view, the neglect of the random nature of concrete would give rise to enormous convergence difficulties (negative

pivots of the factorized tangent stiffness matrix, cyclic convergence behaviour, the risk of converging on an unstable equilibrium path, etc.) associated with the existence of bifurcation points.

With a view to eliminating alternative equilibrium states of numerical and not physical nature, it was decided to introduce a statistical distribution of material parameters. The tensile strength f_t and the fracture energy G_F were considered to be independent random variables following a Gauss distribution truncated at $\bar{X} \pm 3\sigma(X)$, where \bar{X} is the mean value and $\sigma(X)$ is the standard deviation of random variable X . In agreement with experimental findings (Slowik et al., 1993), the coefficients of variation $\sigma(f_t)/\bar{f}_t = 0.1$ and $\sigma(G_F)/\bar{G}_F = 0.2$ were used. Regarding the modulus of elasticity E , it was considered to follow the same distribution as the tensile strength in such a way that the strain corresponding to the peak of the elastic stress-strain constitutive relation remains constant and independent of the location x_i , i.e. $\bar{f}_t/\bar{E} = f_t(x_i)/E(x_i)$ was assumed.

With respect to the adopted unloading strategy, it was assumed that 30% of the maximum attained crack opening remains as residual deformation at zero stress. In this way, both stiffness degradation due to cracking and residual deformation owing to non-congruent crack surfaces can be captured.

Further details concerning other model parameters, the chosen solution procedure and additional assumptions on the material behaviour can be found in Alvaredo (1994). The stability analysis occasionally required to find the location of local snap-backs associated with unstable crack propagation is also described there.

3 Determination of required model parameters

3.1 Direct experimental determination

The experimental determination of the modulus of elasticity, E , belongs to the state-of-the-art (Neville and Brooks, 1987). For instance, following the procedure specified by RILEM (CPC8, 1975), a secant modulus is obtained.

The experimental set-up developed at this Laboratory to carry out deformation-controlled direct tensile tests is described in Slowik (1995). The tensile strength, f_t , the fracture energy, G_F , and the strain softening diagram can be obtained directly from such tests.

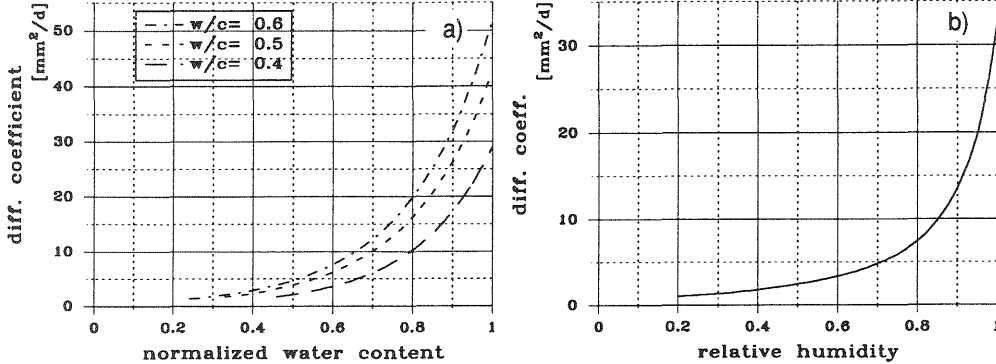


Figure 2: a) relationship between normalized water content and diffusion coefficient for three different water/cement ratios, w/c , after Wittmann et al., 1989; b) relationship between relative humidity and diffusion coefficient for a low performance concrete with $w/c = 0.55$

3.2 Inverse analysis

In order to determine the variation of the diffusion coefficient D with moisture content w , drying tests must be carried out. During these tests, the weight loss is measured as function of time. By assuming a certain shape of the relationship between D and w , in our case an exponential function, a computer program based on the finite difference method and combined with a non-linear least squares fit is used to obtain the diffusion coefficient considering the experimentally determined moisture losses as the target curve (Wittmann et al., 1989). Typical relationships for normal concrete with three different water/cement ratios are shown in Fig. 2a. To obtain the $D-h$ relationship required for the solution of Eq. (1), use is made of the sorption isotherm, i.e. of the curve describing states of hygral equilibrium between the moisture content in the pores of the material, w , and the relative humidity h . The $D - h$ curve obtained in this way for a low performance concrete with a water/cement ratio of 0.55, which was used in the calculations presented in Section 4, is shown in Fig. 2b.

Figs. 3a and 3b illustrate the result of shrinkage tests in which the length change of water cured cylinders made of two different mortars and exposed to an environment at $h_a = 0.45$ is measured as function of the duration of drying. It might be thought that such tests provide the value of the coefficient of shrinkage, α_{sh} in Eq. (4), in a direct and unique way. However, as has been discussed

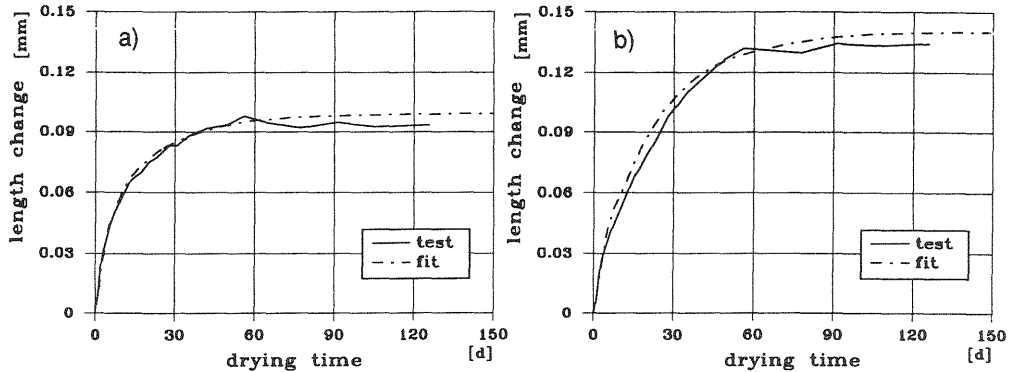


Figure 3: Length change of the axis of mortar cylinders ($\phi = 50 \text{ mm}$, $l = 120 \text{ mm}$) exposed to $h_a = 0.45$ as function of time: a) for $w/c=0.45$; b) for $w/c=0.6$

in Alvaredo (1994) and will be shown in Section 4.1, the observed shrinkage deformation at a certain time is not a material property but the response of the tested specimen to a highly nonlinear state of stress and dependent on the size and geometry of the specimen and on the kinetics of drying.

The easiest way to circumvent the problem posed by the uncertain experimental determination of α_{sh} is to consider it to be a constant, i.e. independent of h , and calculate its value as:

$$\alpha_{sh} = \frac{\Delta l_{t \rightarrow \infty}}{l \Delta h} \quad (5)$$

where $\Delta l_{t \rightarrow \infty}$ is the experimentally determined length change corresponding to hygral equilibrium with the environment, $\Delta h = 1 - h_a$ is the change in relative humidity the initially saturated specimen was exposed to and l is the gauge length. The value of the coefficient of shrinkage determined by Eq. (5) can be considered to describe the average shrinkage characteristics of the material within the range $h_a \leq h \leq 1$. This was the approach followed in Alvaredo (1994) and for the calculations presented in Section 4.

Most authors (Bažant and Chern 1985, Acker et al. 1990) agree, however, that the only rigorous way of determining α_{sh} available so far is by inverse finite element analysis of shrinkage tests. For this purpose, tests similar to those indicated in Figs. 3a and 3b were carried out at two further air relative humidities: $h_a = 0.6$ and 0.75 . The relationship between the coefficient of shrinkage and relative

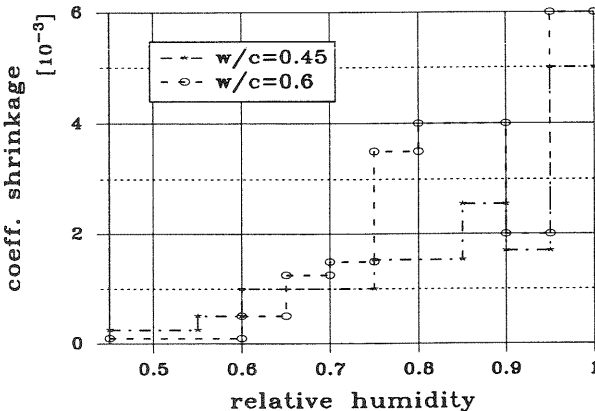


Figure 4: Fitted relationship between the coefficient of shrinkage and relative humidity for two mortar qualities

humidity obtained by fitting shrinkage tests at $h_a = 0.45, 0.6$ and 0.75 is shown in Fig. 4 for mortars with two different water/cement ratios, $w/c = 0.45$ and 0.6 . The fitted $\Delta l = f(t)$ curves obtained for both mortar qualities at $h_a = 0.45$ are also depicted in Figs. 3a and 3b.

Fig. 4 exhibits some interesting characteristics. First of all, the coefficient of shrinkage for relative humidities close to saturation was found to be the highest. This might be explained by the fact that the specimens were cured under water. Capillary underpressure is known to vanish in water filled macropores and, as a result, swelling is observed when the moisture content in the pores is varied from the value corresponding to about 100% relative humidity and water saturation (Pihlajavaara, 1974). This phenomenon is more pronounced for higher water/cement ratios. Most of the water loss observed once capillary underpressure has been reestablished, i.e. for relative humidities slightly below 100%, is from capillary cavities. This water loss causes comparatively little shrinkage. The lower values of α_{sh} for $0.9 \leq h \leq 0.95$ in Fig. 4 can be explained by this mechanism. At lower relative humidities, shrinkage is governed by disjoining pressure (Wittmann, 1977) and, therefore, increases noticeably with decreasing h . Upon further decreasing h , the fitted curves show a more or less steady decrease of α_{sh} , which is in agreement with experimental findings (Pihlajavaara, 1974). It is only at very low relative humidities ($h \leq 0.3$) that the coefficient of shrinkage increases again due to the action of surface free energy.

The fracture mechanics parameters used in the calculations pre-

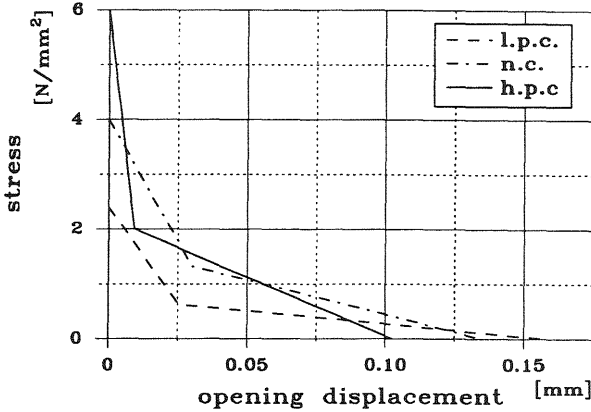


Figure 5: Typical strain softening behaviour of three different concrete qualities

sented in Section 4 and in another contribution to this volume (Alvaredo et al., 1995) were determined from the load-displacement curves obtained as the response of wedge splitting tests. By means of a numerical implementation of the “fictitious crack model” (Pettersson, 1981), the parameters defining a bilinear approximation to the strain softening behaviour were obtained in a trial-and-error manner, so that the numerical force-displacement curve agreed as closely as possible with the experimental one. Fig. 5 illustrates the strain softening behaviour of three different concrete qualities: normal (n.c.), low performance (l.p.c.) and high strength concrete (h.s.c.).

4 Examples

4.1 Axisymmetric geometry

With the aim to emphasize that the observed shrinkage of drying specimens is not a material property but their response to drying and to the stresses induced by drying, a parametric study has been carried out.

Calculations were run for cylinders with a diameter of 150 mm and a length of 480 mm which were exposed to $h_a = 0.44$. The “reference concrete”, with respect to which comparisons were made, was assumed to be characterized by the following properties: the $D - h$ relationship illustrated in Fig. 2b, the coefficient of shrinkage $\alpha_{sh} = 1.5 \cdot 10^{-3} [h^{-1}]$ (for $0 \leq h \leq 1$), $\bar{E} = 40000$ MPa, $\bar{f}_t = 4$ MPa, $\bar{G}_F = 150$ MPa and the shape of the bilinear strain softening dia-

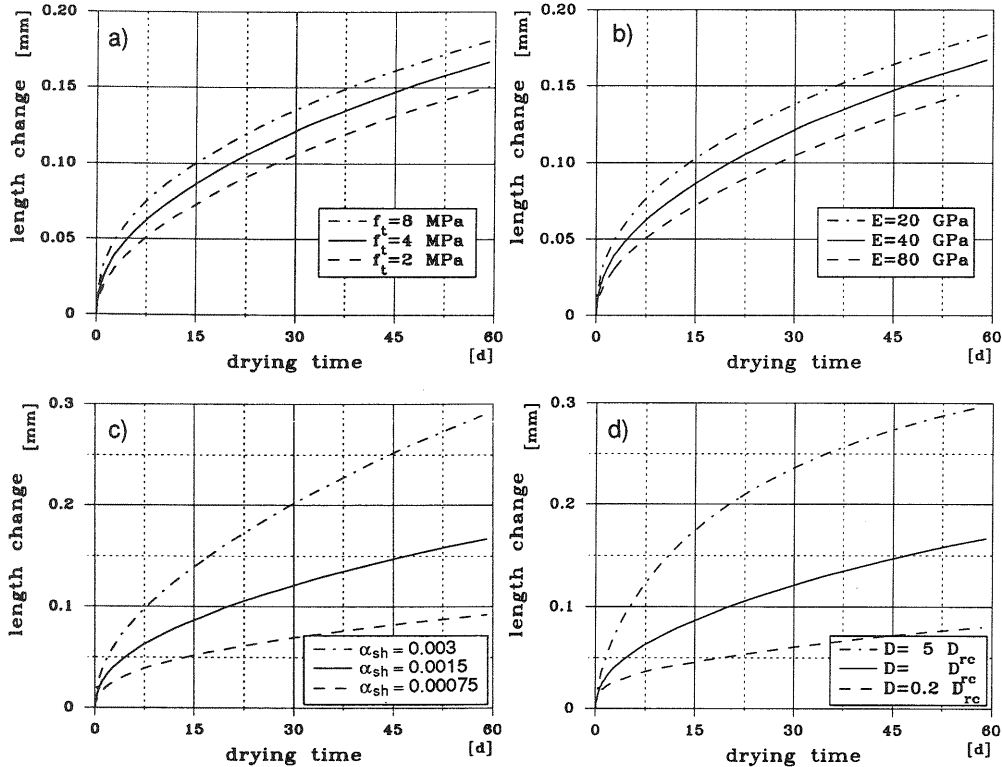


Figure 6: Influence of material properties on change of length induced by drying:
a) f_t ; b) E ; c) α_{sh} ; d) D

gram indicated in Fig. 5 for normal concrete.

The effect of four material properties, f_t , E , α_{sh} and D , on the numerically predicted shrinkage deformation was individually analysed, for which the corresponding properties of the “reference concrete” were multiplied and divided by 2 (f_t , E and α_{sh}) and 5 (D). Figs. 6a to 6d show the evolution with drying time of the length change of a fibre at the drying surface determined between the end-faces. Further results of this parametric study are reported in Alvaredo (1994).

The influence of the tensile strength f_t on shrinkage indicated in Fig. 6a can be explained by the interaction of two competing effects: the tendency of shrinkage to increase with tensile strength vs. more extensive crack formation in the more brittle material with higher f_t resulting in a faster decrease of the rate of shrinkage. It is interesting to note that one of the effects of prolonged curing is an increased f_t at the time of exposure to drying. According to Fig. 6a,

shrinkage can then be expected to increase with the curing period.

In a more flexible material with a lower modulus of elasticity E , the internal restraint against shrinkage deformation exerted by the cross-section is smaller and, as a result, the induced eigenstresses counteracting the deformation due to drying are lower. In addition, crack formation in the zones subjected to tensile eigenstresses, which further reduces shrinkage-induced deformations, is less extensive. For these reasons, as can be seen in Fig. 6b, the change of length increases with decreasing modulus of elasticity. A longer period of curing will result in this case in lower shrinkage.

By looking at Eq. (5), one could expect the change of length to be directly proportional to α_{sh} . This would be approximately so for a linear elastic material. The results in Fig. 6c indicate, however, that more extensive crack formation in the material with higher coefficient of shrinkage reduces the length change due to drying to a considerable extent. Since, owing to the presence of unhydrated cement grains, younger concrete usually exhibits a lower α_{sh} than mature concrete (Alvaredo, 1994), a longer curing period will give rise in this case to higher shrinkage.

When studying the effect of the moisture diffusion coefficient on shrinkage, the $D_{rc} - h$ relationship corresponding to the reference concrete (see Fig. 2b) was just scaled proportionally by 20% and 5 times. The numerical results are shown in Fig. 6d. It is obvious that the main effect of D is related to the kinetics of drying, with lower diffusion coefficients causing a slower evolution of shrinkage with time. Concrete cured for a shorter period is more porous and exhibits a higher diffusion coefficient. For this, shrinkage develops faster than for more mature concrete.

The precise influence of the curing period on shrinkage depends on the effect of several competing mechanisms. It appears, however, that more prolonged curing tends to cause greater shrinkage.

4.2 Free warping

Calculations were run under the assumption of plane stress and symmetry conditions, i.e. the slabs were idealized by means of plates of unit thickness with a length $l/2$. Warping was obtained as the relative vertical displacement between the edge and the symmetry axis. The material was characterized by the set of properties corresponding to the reference concrete in the previous section. In this

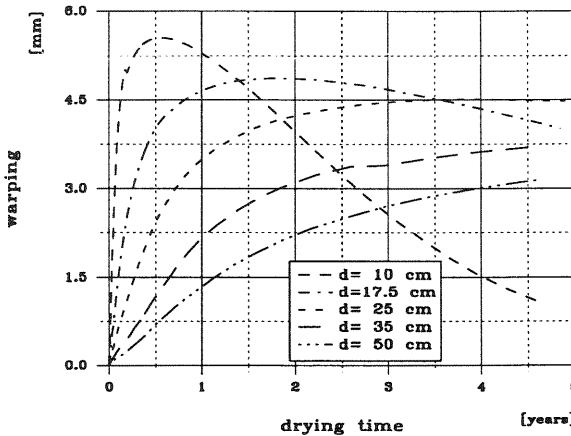


Figure 7: Warping calculated for 6 m long concrete slabs of different depth

case, the dead weight was also taken into consideration in the analysis by applying to all elements in the finite element discretization a downward volume load equal to 2.4 kg/dm^3 , a typical value for the density of normal concrete. The slabs were assumed to be exposed to an environment at $h_a = 0.5$ at their top side. Details of the used finite element mesh and of the consideration of the non-linear boundary conditions acting at the bottom side due to lack of contact with the subbase-subgrade system are given in Alvaredo and Wittmann (1995b).

Fig. 7 shows the warping predicted as a function of drying time for a slab length $l = 6 \text{ m}$ and five different depths: $d = 10, 17.5, 25, 35$ and 50 cm . It can be seen that a change in length is essentially equivalent to a shift in the time required to reach the maximum warping, with deeper slabs deforming more slowly. With respect to the attained maximum, it can be said that it remains almost unaffected by d . For example, an increase in slab depth from 17.5 to 25 cm reduces the maximum warping in 7% only. The slight tendency of the maximum warping to decrease with increasing slab depth is related to the larger magnitude of the tensile eigenstresses induced in deeper members with a larger compression zone and, therefore, with a stiffer cross-section. These higher tensile stresses in deeper members give rise to more extensive cracking; as a consequence thereof, part of the shrinkage deformation, which would otherwise cause warping, is consumed in the opening of fracture process zones.

4.3 Warping prevented by dowels

With the aim to study the stress evolution and the crack formation in drying slabs for which warping is prevented by the action of dowels, the upper corner of the slabs was fixed in the vertical direction. Calculations were carried out under the same model assumptions and hygral boundary conditions as described in the previous section. The geometry was defined by $l/2 = 3$ m and $d = 25$ cm. Three different concrete qualities were considered: l.p.c., n.c. and f.r.c. (fibre reinforced concrete). In all cases, the diffusion properties were described by the $D - h$ relationship depicted in Fig. 2b. The material parameters corresponding to n.c. have been indicated in Section 4.1 as those of the "reference concrete". The remaining two concrete qualities have been characterized as follows: l.p.c. with $\alpha_{sh} = 2.4 \cdot 10^{-3}$ [h^{-1}], $E = 36000$ MPa, $f_t = 2.4$ MPa, $G_F = 80$ N/m and the corresponding shape of the strain softening diagram indicated in Fig. 5 for l.p.c., and f.r.c., identical to n.c. but with a 5-fold higher fracture energy, $G_F = 750$ N/m, due to the addition of fibres.

The vertical reaction at the fixed corner as function of drying time is illustrated in Fig. 8. It is obvious that with increasing severity of cracking the force required to prevent the warping of a drying slab must decrease. The maximum reaction force for l.p.c. is 39% lower and the one for f.r.c. is 29% higher than the corresponding value for n.c. This means that in case warping had not been prevented by means of dowelling, the maximum warping attained by the slab of f.r.c. would have been higher than for the other two qualities. The reason for this behaviour is that the stress transferring capability of the fracture process zones in f.r.c., because of the increased fracture energy of the material, is five times higher than that of the fracture process zones in n.c. The loss of stiffness due to cracking is therefore less and, as a consequence, free warping or the force required to prevent it is higher.

The main advantage of adding fibres is associated with the resulting crack pattern: the pattern of fracture process zones remained fine and diffuse for the whole calculated period of drying and no real cracks appeared in the slab of f.r.c. (Alvaredo and Wittmann, 1995a).

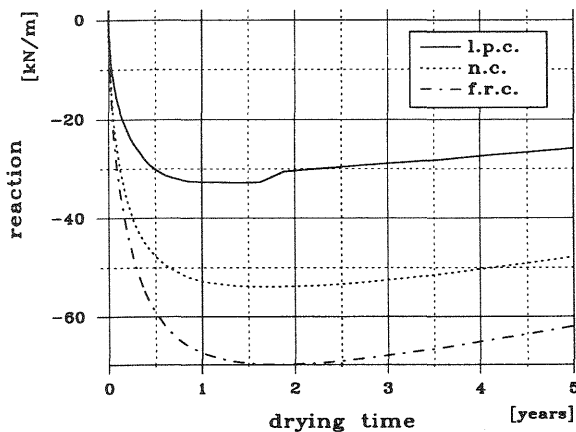


Figure 8: Vertical reaction at the fixed corner of dowelled slabs for three concrete qualities

5 Conclusions

Obviously, the analysis summarized in the foregoing sections is much more complex than the usual treatment of stresses induced by thermal or hygral gradients, i.e. than the plain neglect or the mere empirical consideration of such stresses. It is only by means of a rational approach, however, that the experience gained in practice and by research groups worldwide can be successfully extrapolated to assess the effect of one design variable or technological measure against the effect of others and to meet requirements for high performance.

Engineering intuition based on experience is often misleading in the case of the prediction of structural behaviour under hygral or thermal gradients. General performance of concrete structures, durability in particular, can be noticeably improved if in addition to the conventional static design a rigorous thermal and hygral analysis is carried out.

References

- Acker, P., Mamillan, M. and Buquan, M. (1990) Drying and shrinkage of concrete: the case of massive parts, in **Serviceability and Durability of Construction Materials** (ed B.E. Suprenant), ASCE, New York, U.S.A., 1072-1081.
- Acker, P. and Eymard, R. (1992) Thermal and hygral effects in concrete structures. **Wiss. Zeitschrift Hochschule für Architektur und Bauwesen Weimar**, 3./4./5. Heft, Weimar, Germany, 191-197.

- Alvaredo, A.M. (1994) Drying shrinkage and crack formation. **Building Materials Reports**, 5, Aedificatio, Freiburg, Germany.
- Alvaredo, A.M., Gallo, S. and Wittmann, F.H. (1995) Experimental and numerical study of drying-induced warping of concrete slabs, in this volume.
- Alvaredo, A.M. and Wittmann, F.H. (1995a) Influence of material properties on cracking and warping of a drying concrete ground floor, in **Industrial Floors '95** (ed P. Seidler), Techn. Akademie Esslingen, Esslingen, Germany, 201-207.
- Alvaredo, A.M. and Wittmann, F.H. (1995b) Influence of geometry and boundary conditions on cracking and warping of a drying concrete ground floor, in **Industrial Floors '95** (ed P. Seidler), Techn. Akademie Esslingen, Esslingen, Germany, 209-218.
- Bažant, Z.P. and Najjar, L.J. (1971) Drying of concrete as a nonlinear diffusion problem. **Cem. and Concr. Res.**, 1, 461-473.
- Bažant, Z.P. and Oh, B.H. (1983) Crack band theory for fracture of concrete. **Mat. and Struct.**, 16(93), 155-177.
- Bažant, Z.P. and Chern, J.C. (1985) Concrete creep at variable humidity: constitutive law and mechanism. **Mat. and Struct.**, 18(103), 1-20.
- Concrete Society (1988) Concrete industrial ground floors. Techn. Report No. 34, The Concrete Society, Slough, U.K.
- CPC8 (1975) Modulus of elasticity of concrete in compression. **RILEM Technical Recommendations for the Testing and Use of Construction Materials**, E & FN Spon, London, U.K., 25-27.
- Eisenmann, J. and Leykauf, G. (1990) Effect of paving temperatures on pavement performance. **Proc. 2nd Intern. Workshop on the Theoretical Design of Concrete Pavements**, Sigüenza, Spain, 419-428.
- Gustafsson, P.J. and Hillerborg, A. (1984) Improvements in concrete design achieved through the application of fracture mechanics, in **Applic. of Fracture Mechanics to Cementitious Materials** (ed S.P. Shah), Northwestern Univ., Evanston, Illinois, U.S.A., 667-680.
- Holland, J.A. (1995) Post-tensioned industrial floors in the U.S.A. that minimize open joints and cracks but maximize productivity, in **Industrial Floors '95** (ed P. Seidler), Techn. Akademie Esslingen, Esslingen, Germany, 133-143.
- Hveem, F.N. (1951) Slab warping affects pavement joint performance. **J. ACI**, 22(10), 797-808.
- Mirambell, E. (1990) Temperature and stress distributions in plain concrete pavements under thermal and mechanical load. **Proc. 2nd Intern. Workshop on the Theoretical Design of Concrete Pavements**, Sigüenza, Spain, 121-135.

Neville, A.M. and Brooks, J.J. (1987) **Concrete Technology**. Longman Scientific & Technical, Essex, England.

Petersson, P.E. (1981) Crack growth and development of fracture zones in plain concrete and similar materials. Report TVBM-1006, Lund Institute of Techn., Lund, Sweden.

Pickett, G. (1946) Shrinkage stresses in concrete. **J. ACI**, 17(3), 165-195 & 17(4), 361-398.

Pihlajavaara, S.E. (1965) On the main features and methods of investigation of drying and related phenomena in concrete. PhD Thesis, Univ. of Helsinki, Finland.

Pihlajavaara, S.E. (1974) A review of some of the main results of a research on the ageing phenomena of concrete: effect of moisture conditions on strength, shrinkage and creep of mature concrete. **Cem. and Concr. Res.**, 4, 761-771.

Poblete, M., García, A., David, J., Ceza, P. and Espinosa, R. (1990) Moisture effects on the behaviour of PCC pavements. **Proc. 2nd Intern. Workshop on the Theoretical Design of Concrete Pavements**, Sigüenza, Spain, 429-434.

Rollings, R.S. (1989) Developments in the Corps of Engineers rigid airfield design procedures. **Proc. 4th Intern. Conf. on Concrete Pavement Design and Rehabilitation**, Purdue Univ., West Lafayette, Indiana, U.S.A., 405-418.

Saxena, S.K. and Dounias, G.T. (1986) Mechanical and environmental stresses in continuously reinforced concrete pavements, in **Concrete Pavement Design and Performance**, Transportation Research Record 1099, Washington D.C., U.S.A., 12-22.

Silfwerbrand, J. (1990) Control of cracking in continuously reinforced concrete pavements - research needs. **Proc. 2nd Intern. Workshop on the Theoretical Design of Concrete Pavements**, Sigüenza, Spain, 264-279.

Slowik, V., Alvaredo, A.M. and Wittmann, F.H. (1993) Experimental and numerical investigation into the probabilistic character of crack growth, in **Numerical Models in Fracture Mechanics of Concrete** (ed F.H. Wittmann), Balkema, Rotterdam, The Netherlands, 223-231.

Slowik, V. (1995) Beiträge zur experimentellen Bestimmung bruchmechanischer Materialparameter von Betonen, 2nd Edition. **Building Materials Reports**, 3, Aedificatio, Freiburg, Germany.

Wittmann, F.H. (1977) Grundlagen eines Modells zur Beschreibung charakteristischer Eigenschaften des Betons. **Deutscher Ausschuss für Stahlbeton**, Heft 290, 43-101.

- Wittmann, F.H. and Roelfstra, P.E. (1980) Total deformation of loaded drying concrete. **Cem. and Concr. Res.**, 10, 601-610.
- Wittmann, F.H. (1995) Influence of drying induced damage on the hygral diffusion coefficient, in this volume.
- Wittmann, X., Sadouki, H. and Wittmann, F.H. (1989) Numerical evaluation of drying test data. **Trans. 10th Intern. Conf. on Structural Mechanics in Reactor Technology**, Q, 71-79.
- Zollinger, D.G. and Barenberg, E.J. (1989) A mechanistic based design procedure for jointed concrete pavements. **Proc. 4th Intern. Conf. on Concrete Pavement Design and Rehabilitation**, Purdue Univ., West Lafayette, Indiana, U.S.A., 75-97.

